



Cite this: *RSC Adv.*, 2024, **14**, 19185

Received 21st March 2024
 Accepted 6th June 2024

DOI: 10.1039/d4ra02177k
rsc.li/rsc-advances

Self-assembly and antimicrobial activity of cationic gemini surfactants containing triazole moieties†

Karima Amel Mechken, ^{ab} Mohammed Menouar,^c Zahera Talbi,^b Salima Saidi-Besbes ^{*a} and Moulay Belkhodja^c

1,2,3-Triazole-based gemini bis-quaternary ammonium surfactants with varying hydrophobic chain length and ethylene or butylene spacers were synthesized and characterized. Their surface and aggregation properties were analyzed using tensiometry and conductometry. The gemini surfactants showed significantly lower CMC values compared to their single-tail counterparts and conventional gemini surfactants described in the literature. The micellization and surface adsorption processes in water can be tailored according to the hydrophobic chain and the spacer length and were substantially improved by the presence of the heterocycle. These surfactants are active against various Gram-positive and Gram-negative bacterial stains, as well as fungi. The gemini surfactant with tetradecyl chain and ethylene spacer (Bis 14–2–14) exhibited the highest activity against all investigated microbial strains.

1 Introduction

Gemini surfactants, also referred to as dimeric surfactants, consist of two hydrophilic heads and two hydrophobic chains that are connected by a rigid or flexible spacer.¹ Over the last two decades, they have attracted particular interest in different fields including material sciences, wastewater remediation,^{2,3} surface treatment,^{4,5} catalysis,^{6,7} analytical separation, solubilization and flotation processes⁸ and paint additive industry.^{9,10} Compared to conventional single-tail surfactants, they are more effective and can often attain much lower surface tension, critical micellar concentration and Kraft point values.^{11–13} Additionally, they have favorable interfacial and viscoelastic properties, as well as a rock wetting ability, making them the subject of numerous studies in the field of enhanced oil recovery (EOR) to replace conventional fluids.^{14,15}

In the biomedical and biotechnological fields, numerous studies highlighted the potential of gemini surfactants as templates for the preparation of nanoparticles and self-assembled systems for the encapsulation and controlled delivery of drugs and other active ingredients.¹⁶ Furthermore, the interaction of gemini surfactants with multiple biological

targets such as serum albumin proteins,^{17,18} membrane lipids and oligosaccharides has been emphasized.¹⁹

From a chemical perspective, several types of gemini surfactants have been reported, including imidazolium salts,²⁰ pyridinium salts,²¹ pyrrolidinium salts,²² amino acids²³ and benzene sulfonates.²⁴ Various structural variations have been described for the spacer which can include a short²⁵ or long alkyl chain,²⁶ a rigid (stilbene, benzene)²⁷ or flexible (alkyl or alkoxy) chain,²⁸ a polar (polyether)²⁹ or non-polar (aliphatic, aromatic) chain.³⁰ Moreover, the polar group can be cationic (quaternary ammonium), anionic (phosphate, sulfate, carboxylate) or nonionic (polyether, sugar).³¹ While most gemini surfactants have two similar hydrophobic chains, asymmetric derivatives are also possible.³²

We recently designed single-chain triazole-based surfactants with remarkable surface properties and antimicrobial performances against several microorganisms, including Gram-positive and Gram-negative bacteria as well as fungus. Lower minimum inhibitory concentration (MIC) values were reached by these compounds as compared to benzalkonium chloride (BAC) derivatives commonly applied for hospital disinfection.¹³ Gemini surfactants are commonly regarded as more promising than monomeric surfactants in terms of aggregation and biological properties. However, the study of structure–activity relationships is not always obvious, and the literature often reports fragmentary and contradictory results, particularly regarding the effect of dimeric structures on the antimicrobial properties. The aim of this work is to expand our understanding of triazolic-based surfactant systems and investigate the behavior of related gemini structures that contain two triazole synthons and two quaternary ammonium units in the self-assembly process and antimicrobial properties. A series of

^aUniversité Oran1, Laboratoire de Synthèse Organique Appliquée (LSOA), Département de Chimie, Faculté des Sciences Exactes et Appliquées, BP 1524 ELMnaouer, 31000 Oran, Algeria. E-mail: saidi.salima@univ-oran1.dz

^bUniversité Oran 2, Institut de Maintenance et de Sécurité Industrielle, 31000 Oran, Algeria

^cUniversité Oran 1, Laboratoire de Biotoxicologie Expérimentale, Biodépollution et Phytoremédiation, 31000, Oran, Algeria

† Electronic supplementary information (ESI) available. See DOI: <https://doi.org/10.1039/d4ra02177k>



symmetrical dimeric quaternary ammonium salts bearing 4-alkyl-1*H*-1,2,3-triazole side groups and varying spacer chain length were synthetized and characterized. Their micellar and interfacial behaviors were investigated by tensiometry and conductometry while their biological activities were determined by bacterial growth inhibition assays.

2 Experimental section

2.1. Materials and methods

1-Bromoocane, 1-bromodecane, 1-bromododecane, 1-bromo-tetradecane, 1-bromohexadecane, *N,N,N',N'*-tetramethylmethylethylenediamine, *N,N,N',N'*-tetramethyl-1,4-butanediamine, propargyl bromide, sodium azide, copper acetate and sodium ascorbate were supplied by Sigma-Aldrich (Algeria) and used as received.

The alkylazides (**1a–e**) were synthesized following reported protocols^{13,33} by the reaction of 1-bromoalcano with sodium azide and sodium iodide in DMF.

Melting temperatures were obtained using a Kofler benchtop equipment (Leica–Wagner & Munz, Germany), which was pre-calibrated before each measurement.

¹H NMR and ¹³C NMR analyses were performed on a BRUKER AC 300P spectrometer (Wissembourg, France) at 300 and 75 MHz frequencies, respectively. Chemical shifts (δ) are given in parts per million relative to tetramethylsilane (TMS) and coupling constants (J) are expressed in Hz.

High resolution mass spectroscopy (HRMS) has been carried out using SYNAPT instrument, waters in ESI⁺ mode (0.1% formic acid in 1:1 water/methanol). Leucine enkephalin (555.2693 g mol⁻¹) was used as an internal standard.

2.1.1. Synthesis of bispropargyl diammonium bromide intermediates (BisP-s), *s* = 2, 4. Propargyl bromide (1 g, 8.40 mmol) was dissolved in anhydrous acetonitrile (30 mL), followed by the dropwise addition of (3.82 mmol) of *N,N,N',N'*-tetramethylmethylethylenediamine or *N,N,N',N'*-tetramethyl-1,4-butanediamine. The solution was stirred at room temperature for 48 hours. The mixture was then cooled to 0 °C and the obtained precipitate was filtered, washed three times with acetonitrile, then with hexane and, dried under vacuum.

N,N,N',N'-tetramethyl-*N,N'*-dipropargyl-ethane-1,2-diammonium bromide (**BisP-2**) white solid, yield: 59%, m.p. 240 °C. ¹H NMR (300 MHz, CD₃OD) δ (ppm) 3.40 (s, 12*H*), 3.68 (t, 2*H*, J = 2.9 Hz), 4.19 (s, 4*H*), 4.57 (m, 4*H*). ¹³C NMR (75 MHz, CD₃OD) δ (ppm) 50.9, 55.9, 59.3, 71.6, 79.5.

N,N,N',N'-tetramethyl-*N,N'*-dipropargyl-butane-1,4-diammonium bromide (**BisP-4**): yellow solid, yield: 76%, m.p. 265 °C. ¹H NMR (300 MHz, CD₃OD) δ (ppm) 1.95 (m, 4*H*), 3.26 (s, 12*H*), 3.59 (t, 2*H*, J = 2.9 Hz), 3.62 (m, 4*H*), 4.44 (m, 4*H*). ¹³C NMR (75 MHz, CD₃OD) δ (ppm) 22.7, 50.9, 56.8, 63.4, 69.9, 80.8.

2.1.2. Synthesis of gemini surfactants (Bis n-s-n). A solution of bisammonium intermediate (**BisP-s**) (1.05 mmol), alkylazide (2.1 mmol), copper acetate (0.055 g, 0.3 mmol) and sodium ascorbate (0.1 g, 0.5 mmol) in acetonitrile (30 mL) was heated at 60 °C for 3 days. After evaporation of the solvent, the resulting residue was solubilized in chloroform and filtered to remove the catalyst. The solvent was then evaporated under

reduced pressure and the crude product was triturated three times with hexane then washed with petroleum ether.

The gemini surfactants will be referred to as **Bis n-s-n** where *s* is the number of carbons in the spacer arm (*s* = 2, 4) and *n* is the number of carbons in the hydrophobic side chains C_{*n*}H_{2*n*+1} (*n* = 8, 10, 12, 14 or 16).

Bis 8-2-8: purple solid, yield: 64%, m.p. 56 °C. ¹H NMR (300 MHz, CDCl₃) δ (ppm) 0.87 (t, 6*H*, J = 7.0 Hz), 1.25 (m, 20*H*), 1.90 (m, 4*H*), 3.48 (s, 12*H*), 4.40 (m, 8*H*), 5.07 (s, 4*H*), 8.59 (s, 2*H*). ¹³C NMR (75 MHz, CDCl₃) δ (ppm): 14.1, 22.6, 29, 29, 1, 30.1, 31.7, 50.9, 51.7, 55.9, 58.9, 128.8, 134.5. HRMS (ESI⁺): *m/z* 583.3810 (calculated), 583.3811 (found), [M–HBr].

Bis 10-2-10: brown solid, yield: 69%, m.p. 61 °C. ¹H NMR (300 MHz, CDCl₃) δ (ppm): 0.87 (t, 6*H*, J = 6.9 Hz), 1.27 (m, 28*H*), 1.89 (m, 4*H*), 3.49 (s, 12*H*), 4.39 (m, 8*H*), 5.09 (s, 4*H*), 8.60 (s, 2*H*). ¹³C NMR (75 MHz, CDCl₃) δ (ppm): 14.1, 22.6, 26.6, 29.1, 29.3, 29.5, 29.7, 30.1, 32.0, 50.9, 51.6, 56.0, 58.8, 128.8, 134.6. HRMS (ESI⁺): *m/z* 639.493 (calculated), 639.4437 (found), [M–HBr].

Bis 12-2-12: yellow solid, yield: 73%, m.p. 63 °C. ¹H NMR (300 MHz, CDCl₃) δ (ppm): 0.88 (t, 6*H*, J = 6.9 Hz), 1.26 (m, 36*H*), 1.91 (m, 4*H*), 3.50 (s, 12*H*), 4.40 (m, 8*H*), 5.13 (4*H*, s), 8.61 (2*H*, s). ¹³C NMR (75 Hz, CDCl₃) δ (ppm): 14.1, 22.7, 26.7, 29.1, 29.3, 29.4, 29.5, 29.6, 29.7, 30.9, 32.0, 50.9, 51.7, 56.2, 59.1, 128.8, 134.7. HRMS (ESI⁺): *m/z* 695.5064 (calculated), 695.5063 (found), [M–HBr].

Bis 14-2-14: brown solid, yield: 78%, m.p. 68 °C. ¹H NMR (300 MHz, CDCl₃) δ (ppm): 0.88 (t, 6*H*, J = 6.8 Hz), 1.24 (m, 44*H*), 1.9 (m, 4*H*), 3.50 (s, 12*H*), 4.38 (m, 8*H*), 5.09 (s, 4*H*), 8.59 (s, 2*H*). ¹³C NMR (75 MHz, CDCl₃) δ (ppm): 14.14, 22.7, 26.6, 29.16, 29.4, 29.6, 29.71, 29.77, 30.2, 31.9, 50.9, 51.7, 56.15, 58.9, 128.8, 134.5. HRMS (ESI⁺): *m/z* 751.5689 (calculated), 751.5689 (found), [M–HBr].

Bis 16-2-16: brown solid, yield: 75%, m.p. 70 °C. ¹H NMR (300 MHz, CDCl₃) δ (ppm): 0.88 (t, 6*H*, J = 6.8 Hz), 1.25 (m, 52*H*), 1.91 (m, 4*H*), 3.50 (s, 12*H*), 4.38 (m, 8*H*), 5.10 (s, 4*H*), 8.60 (s, 2*H*). ¹³C NMR (75 MHz, CDCl₃) δ (ppm): 14.1, 22.7, 26.6, 28.8, 29.1, 29.4, 29.5, 29.7, 29.8, 30.2, 31.9, 50.9, 51.6, 56.2, 58.8, 128.7, 134.6.

Bis 8-4-8: red solid, yield: 71%, m.p. 64 °C. ¹H NMR (300 MHz, CDCl₃) δ (ppm): 0.89 (t, 6*H*, J = 6.9 Hz), 1.24 (m, 20*H*), 1.33 (m, 4*H*), 1.92 (m, 4*H*), 3.32 (s, 12*H*), 3.93 (m, 4*H*), 4.45 (t, 4*H*, J = 6.9 Hz), 5.02 (s, 4*H*), 8.76 (s, 2*H*). ¹³C NMR (75 MHz, CDCl₃) δ (ppm): 14.1, 20.1, 22.7, 26.8, 29.2, 29.3, 30.6, 31.8, 50.9, 51.4, 58.4, 63.4, 128.5, 135.9. HRMS (ESI⁺): *m/z* 611.4126 (calculated), 611.4125 (found), [M–HBr].

Bis 10-4-10: brown solid, yield: 74%, m.p. 66 °C. ¹H NMR (300 MHz, CDCl₃) δ (ppm): 0.87 (t, 6*H*, J = 6.9 Hz), 1.25 (m, 28*H*), 1.35 (m, 4*H*), 1.90 (m, 4*H*), 3.46 (s, 12*H*), 3.95 (m, 4*H*), 4.39 (t, 4*H*, J = 6.9 Hz), 5.09 (s, 4*H*), 8.60 (s, 2*H*). ¹³C NMR (75 MHz, CDCl₃) δ (ppm): 14.1, 20.1, 22.7, 26.7, 29.1, 29.3, 29.6, 30.4, 31.9, 50.9, 51.3, 58.5, 63.2, 128.3, 135.0. HRMS (ESI⁺): *m/z* 667.4750 (calculated), 667.4753 (found), [M–HBr].

Bis 12-4-12: orange solid, yield: 79%, m.p. 69 °C. ¹H NMR (300 MHz, CDCl₃) δ (ppm): 0.89 (t, 6*H*, J = 6.9 Hz), 1.26 (m, 36*H*), 1.33 (m, 4*H*), 1.95 (m, 4*H*), 3.36 (s, 12*H*), 3.90 (m, 4*H*), 4.43 (t, 4*H*, J = 6.9 Hz), 4.99 (s, 4*H*), 8.80 (s, 2*H*). ¹³C NMR (75 MHz, CDCl₃) δ (ppm): 14.1, 20.1, 22.7, 26.7, 29.2, 29.4, 29.7, 30.3, 31.9, 50.9,



51.1, 58.7, 63.4, 128.8, 134.9. HRMS (ESI⁺): *m/z* 723.5376 (calculated), 723.5378 (found), [M-HBr].

Bis 14-4-14: green solid, yield: 83%, m.p. 71 °C. ¹H NMR (300 MHz, CDCl₃) δ (ppm): 0.89 (t, 6H, *J* = 6.9 Hz), 1.27 (m, 44H), 1.34 (m, 4H), 1.95 (m, 4H), 3.36 (s, 12H), 3.92 (m, 4H), 4.43 (t, 4H, *J* = 6.9 Hz), 5.01 (s, 4H), 8.89 (s, 2H). ¹³C NMR (75 MHz, CDCl₃) δ (ppm): 14.1, 19.9, 22.7, 26.6, 29.0, 29.3, 29.5, 29.6, 29.6, 29.7, 30.3, 31.9, 50.9, 51.2, 58.6, 63.8, 128.8, 134.9. HRMS (ESI⁺): *m/z* 779.6002 (calculated), 779.6002 (found), [M-HBr].

Bis 16-4-16: green solid, yield: 70%, m.p. 73 °C. ¹H NMR (300 MHz, CDCl₃) δ (ppm): 0.89 (t, 6H, *J* = 6.9 Hz), 1.26 (m, 52H), 1.34 (m, 4H), 1.95 (m, 4H), 3.36 (s, 12H), 3.90 (m, 4H), 4.43 (t, 4H, *J* = 6.9 Hz), 4.99 (s, 4H), 8.89 (s, 2H). ¹³C NMR (75 MHz, CDCl₃) δ (ppm): 14.1, 20.1, 22.7, 26.6, 28.8, 29.2, 29.4, 29.5, 29.6, 29.7, 29.8, 30.2, 31.9, 50.9, 51.4, 58.8, 63.3, 128.7, 135.1.

2.2. Surface tension measurements

Surface tensions of synthesized surfactants were determined by the Wilhelmy plate method at 25 °C by using a GIBERTINI K100 tensiometer. The apparatus was calibrated before each series of measurements. Demineralized water with a surface tension of 72 mN m⁻¹ was used to prepare surfactant solutions with a concentration ranging from 10⁻⁹ to 10⁻² M.

2.3. Conductivity measurements

Conductivities were recorded at 25 °C using an OHAUS STARTER 300C conductimeter. Deionized water with a conductivity of 0.09 μS was used to prepare surfactant solutions. The CMCs were evaluated by identifying the breakpoint on conductivity *versus* surfactant concentration curves.

2.4. Antimicrobial activities

The ability of the synthesized surfactants to inhibit the proliferation of five pathogenic microorganisms was evaluated by the agar diffusion method.³⁴ Two Gram-positive bacteria strains *Staphylococcus aureus* (ATCC25923) and *Bacillus subtilis sub spizizeni* (ATCC 6633), two Gram-negative bacteria strains *Pseudomonas aeruginosa* (ATCC 27853) and *Escherichia coli* (ATTC 2592), and a fungal strain *Aspergillus sniger* (ATCC 16404) were used in this study. The surfactant's antimicrobial activity was evaluated using the Minimum Inhibitory Concentration (MIC), which corresponds to the lowest concentration of the surfactant solution where no visible *in vitro* microorganism growth occurs after incubation; as well as the Minimum Bactericidal Concentration (MBC), which is the lowest concentration of antimicrobial agent capable of inactivating over 99.9% of the inoculum. The BMC/MIC ratio indicates whether the molecule has a bactericidal or bacteriostatic effect.

To determine the MIC of the investigated compounds, surfactant solutions ranging from 5 to 500 μg mL⁻¹ were prepared by dissolving the appropriate quantity of surfactant in doubly distilled and sterilized water. The solutions were then filtered through a 0.45 μm Millipore filter. The inoculums for each microbial strains were prepared by incubating the micro-organisms in nutrient bacterial (24 h at 37 °C) and mycological

broths (72 h at 30 °C). The cultures were then diluted to 10⁸ cfu mL⁻¹.

In a typical experiment, 100 μL of inoculum was seeded onto the surface of the Muller-Hinton medium in Petri dishes. The Petri dishes were sealed and left at room temperature for 20 minutes. Then, wells with a diameter of 4–5 mm were cut into the seeded agar layer. A microdrop of MH-agar was poured into the bottom of each well to clog it, and a volume of 25 μL of each concentration of the tested product was added. After 25 minutes of diffusion, the cultures were incubated in an oven at 37 °C for 24 hours for the antibacterial tests and at 30 °C for 72 hours for the antifungal tests. The MIC value was determined by visually inspecting the growth inhibition of each well in comparison to the negative control well (without any test compound). A positive control was also made with chloramphenicol (30 μg per disc). Experiments were repeated three times for each concentration.

BMC was determined by counting surviving bacteria in the presence of antimicrobial agent concentrations above MIC. The liquid dilution method was used for this purpose: 0.5 mL of surfactant solution with a concentration of 2MIC, 4MIC, 8MIC or 16MIC was added to 0.5 mL of sterilized nutrient broth in a hemolysis tubes. 10 μL of the tested microbial inoculum was then added to each concentration. 50 μL aliquots of the resulting media were then poured into Petri dishes containing a layer of Mueller-Hinton agar and incubated under the same conditions as previously reported. The agar plates were observed for the presence or absence of bacteria before and after incubation. The bactericidal or bacteriostatic effects were assessed using the BMC/MIC ratio.

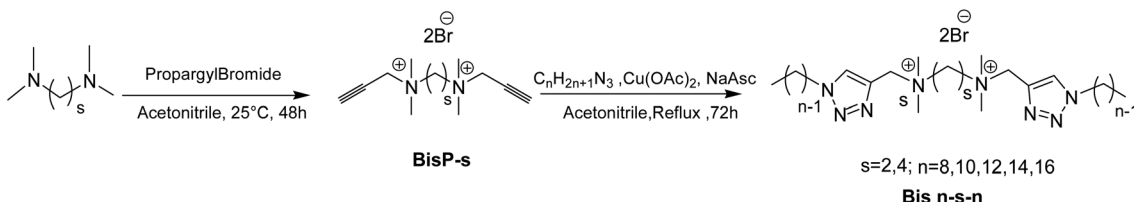
3 Results and discussion

3.1. Synthesis

Two series of gemini triazolic cationic surfactants with either an ethylene or butylene spacer and a hydrophobic chain length ranging from octyl to hexadecyl were synthesized by the two-step synthetic strategy shown in Scheme 1. Firstly, the bispropargyl intermediates **BisP-s** (*s* = 2–4) were prepared through the Menshutkin reaction by the quaternization of the commercial tertiary diamines, *N,N,N',N'*-tetramethyl-1,2-diaminoethane and *N,N,N',N'*-tetramethyl-1,2-diaminobutane with an excess of propargyl bromide. The compounds were obtained with moderate yields even after increasing the propargyl bromide content and reaction's time and temperature. In the second step, a copper-catalyzed 1,3-dipolar cycloaddition (CuAAC) reaction between **BisP-s** intermediates and alkylazides was carried out in the presence of copper acetate and sodium ascorbate. These reagents enable an economical and effective *in situ* reduction of Cu(II) to Cu(I) and lead to the formation of 1,4-disubstituted 1,2,3-triazoles in a regioselective manner with good yields and high purity.

The structures of the prepared ammonium surfactants were confirmed using ¹H and ¹³C NMR. The regioselectivity of the cycloaddition reaction was verified in the ¹H NMR spectra by the presence of a single singlet at 8.59 ppm related to the H-5 proton of the triazole cycle and in the ¹³C NMR spectra with





Scheme 1 Synthetic scheme of the triazolic gemini surfactants **Bis n-s-n**.

the occurrence of two peaks at 134.5 ppm and 128.8 ppm corresponding to the two sp^2 carbons of the triazole cycle.

3.2. Surface activity

Surface properties and self-organization ability of the synthesized triazole based gemini surfactants in aqueous solution were assessed by tensiometry and conductimetry. Several parameters were determined including critical micellar concentrations, surface tensions and free energies of micellization in the aim to highlight relationships between the surfactant molecular structures, and mainly the hydrophobic chain and spacer lengths, and the surface properties. Surfactant solutions of various concentrations were prepared for this purpose using deionized water.

3.2.1. Surface tension. The critical micellar concentrations (CMC) were calculated from the breakpoint of the curves of equilibrium surface tensions (γ), obtained from the Wilhelmy method, *versus* the logarithm of surfactant concentrations.^{13,35} Fig. 1 shows a typical example of the obtained curves for **Bis 8-s-8** series. The absence of a minimum near the breaking point suggests that the compounds are sufficiently pure. The critical micellar concentrations and surface tension values of all synthesized gemini surfactants are listed in Table 1.

It is apparent from the data in Table 1 that the cationic gemini surfactants exhibit very low CMC values and tend to

associate at much lower concentrations than the conventional monomer counterparts described in a previous work.¹³ The CMC values range from 0.0488 to 0.0079 mM for **Bis n-2-n** and from 0.0809 to 0.0014 mM for **Bis n-4-n** while they didn't exceed 0.791–0.037 mM for the reported *N*-(1-alkyl-1-*H*-1,2,3-triazol-4-ylmethyl)-*N,N,N*-triethylammonium bromide (CnTzTEA) monomeric analogues.¹³ A reduction of almost 10 to 25 times is thus achieved by gemini surfactants indicating a much better surface activity. This behavior is related to the greater hydrophobic character of gemini surfactants due to the presence of two hydrophobic chains.^{35–37}

Another interesting finding of this study is the positive impact of the 1,2,3-triazole unit on the micellization ability of studied surfactants. Indeed, for the same hydrophobic chain and spacer lengths, the CMC values of triazole based geminis (**Bis n-2-n** and **Bis n-4-n**) are much lower than those reported for analogous hydrocarbon based gemini surfactants *n-s-n*. For instance, the CMCs of geminis with terminal dodecyl chains 12–4–12 and 12–2–12 are equal to 1.28 and 0.9 mM (ref. 11) while they reach 0.0431 and 0.0253 mM for **Bis 12-4-12** and **Bis 12-2-12**, respectively. Similarly, 14–*s*–14 surfactants show much higher CMC values (0.16 mM for *s* = 2 and 0.1 mM for *s* = 4 (ref. 38)) as compared with **Bis 14-2-14** (0.0099 mM) and **Bis 14-4-14** (0.0112 mM), respectively. This result indicates that the 1,2,3-triazole rings affects the surfactant's surface properties and promote the micellization process.

Fig. 2 shows the evolution of CMC values as a function of the number of carbons (*n*) in the hydrophobic chains. As expected, a gradual decrease of CMCs with the lengthening of the alkyl chain is observed for both series of geminis. This result is related to the increase of the chain's hydrophobicity which facilitates the aggregation of surfactant molecules in aqueous solution. Overall, the short spacer geminis **Bis n-2-n** exhibit lower CMCs as compared to **Bis n-4-s** series probably due to a better orientation of the hydrophobic chains achieved through the fully extended ethylene spacer. Similar results have been reported in previous studies.¹¹ The opposite behavior was obtained for hexadecyl chain-based surfactants (*n* = 16) since the compound **Bis 16-4-16** showed a lower CMC as compared to **Bis 16-2-16**. The steric hindrance induced by long hydrophobic chains may disfavor the self-assembly of short spacer molecules. This constraint will be attenuated by a more flexible butyl spacer.

Another fundamental property of a surfactant is its ability to adsorb at the water-air interface and reduce the surface tension of water. All of the studied surfactants exhibited low surface

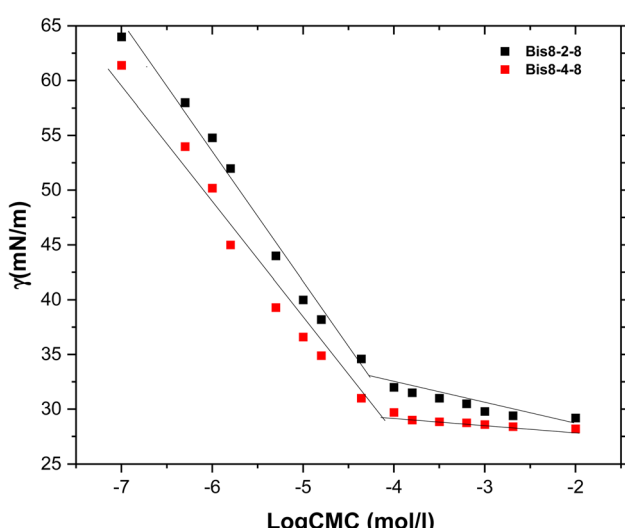


Fig. 1 Equilibrium surface tension (γ) versus the logarithm of **Bis 8-s-8** surfactant concentration curves.



Table 1 Physicochemical parameters of gemini surfactants in aqueous solution

| Surfactant | CMC ^a (mM) | CMC ^b (mM) | γ_{CMC} (mN m ⁻¹) | $P_{C_{20}}$ | CMC/C ₂₀ | Γ_{Max} (μmol m ⁻²) | A_{min} (Å) | β | ΔG_{mic} (kJ mol ⁻¹) |
|---------------------|-----------------------|-----------------------|--------------------------------------|--------------|---------------------|--|---------------|---------|--|
| <i>n</i> = 2 | | | | | | | | | |
| Bis 8-2-8 | 0.0488 | 0.0475 | 34.07 | 5.98 | 46.48 | 0.629 | 263.95 | 0.59 | -37.83 |
| Bis 10-2-10 | 0.0448 | 0.0410 | 34.26 | 5.94 | 38.99 | 0.650 | 246.74 | 0.62 | -39.44 |
| Bis 12-2-12 | 0.0252 | 0.0247 | 34.06 | 6.01 | 25.57 | 0.745 | 222.75 | 0.72 | -44.24 |
| Bis 14-2-14 | 0.0099 | 0.0095 | 35.90 | 6.40 | 25.09 | 0.672 | 246.81 | 0.88 | -53.26 |
| Bis 16-2-16 | 0.0079 | 0.0073 | 39.95 | 6.07 | 9.32 | 0.727 | 228.40 | 0.80 | -51.04 |
| <i>n</i> = 4 | | | | | | | | | |
| Bis 8-4-8 | 0.0809 | 0.0698 | 34.14 | 5.79 | 50.14 | 0.614 | 270.26 | 0.42 | -31.00 |
| Bis 10-4-10 | 0.0618 | 0.0638 | 36.24 | 5.53 | 21.26 | 0.694 | 239.18 | 0.70 | -40.72 |
| Bis 12-4-12 | 0.0489 | 0.0551 | 40.39 | 5.30 | 9.76 | 0.685 | 242.07 | 0.86 | -46.65 |
| Bis 14-4-14 | 0.0112 | 0.0113 | 42.03 | 5.73 | 6.01 | 0.748 | 221.74 | 0.88 | -52.77 |
| Bis 16-4-16 | 0.0014 | 0.0011 | 43.75 | 6.37 | 3.29 | 0.931 | 178.31 | 0.63 | -49.83 |

^a Measured by tensiometry. ^b Measured by conductometry.

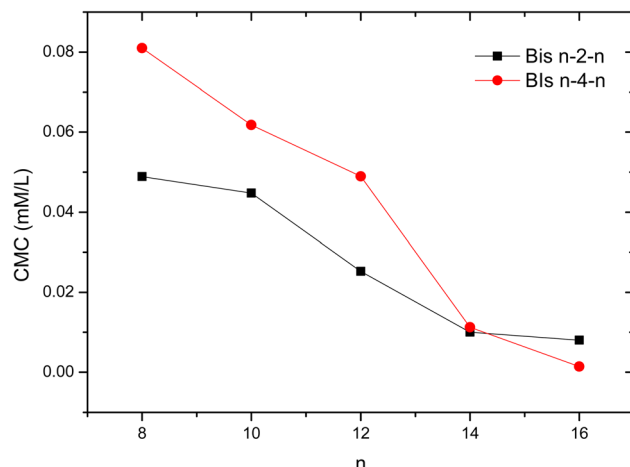


Fig. 2 Evolution of CMC values of gemini surfactants with the length of the alkyl chains.

tensions, with **Bis 8-8-8** reaching a minimum of 34 mN m⁻¹. Surface tensions were found to be closely dependent on the length of the hydrophobic chains and the spacer, increasing as these chains lengthened (Fig. 3).

In order to better understand the behavior of investigated surfactants in aqueous solutions, the CMC/C₂₀ ratio were determined where C₂₀ is the surfactant concentration that reduces the surface tension of water by 20 mN m⁻¹. This parameter is commonly applied to assess the surfactant's effectiveness and to correlate the structural parameters with the processes of micellization and adsorption. As the CMC/C₂₀ values increases, the surfactant will be more effectively adsorbed at the air–water interface to the detriment of the formation of micelles.

Fig. 4 shows that the effectiveness of the adsorption of **Bis 8-8-8** exceeds that of longer chain analogous suggesting the greater tendency for the former geminis to adsorb at the interface and decrease the surface tension of water. Conversely, the micellization process is more favored with the lengthening of the hydrophobic chains and spacer.

The maximum surface concentration excess (Γ_{max}) and the minimum area occupied by a surfactant at the air–water interface (A_{min}) were also calculated using the following Gibbs adsorption equations.³⁹ The aim is to evaluate the degree of molecular organization at the interface.

$$\Gamma_{max} = \frac{-1}{n \times 2.303RT} \left(\frac{d\gamma}{d \log C} \right)_T$$

$$A_{min} = \frac{1}{\Gamma_{max} N_A}$$

where, d γ /d log C is the descending section slope of γ – log C curves near the CMC, T is the temperature in Kelvin, R is the gas constant ($R = 8.314 \text{ J mol}^{-1} \text{ K}^{-1}$), N_A is Avogadro constant, The constant n is related to the number of species present at the air–water interface. For gemini surfactants, n equals 3.

Overall, the A_{min} values decrease as the number of carbons in the hydrophobic chains increases, reflecting a more compact assembly of molecules at the water–air interface (Fig. 5). An opposite behavior was noticed for **Bis n-2-n** beyond twelve

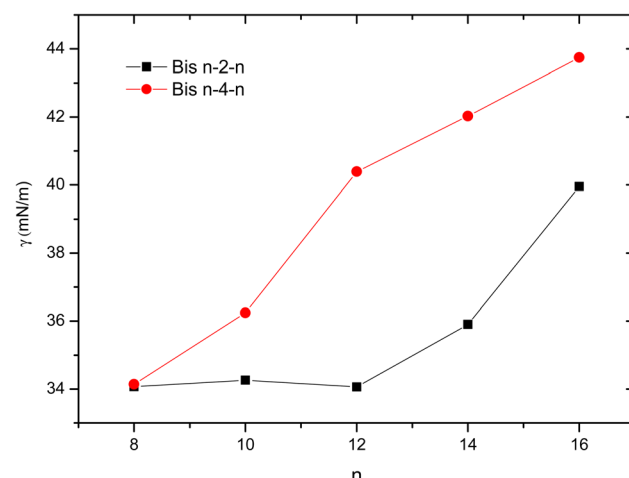
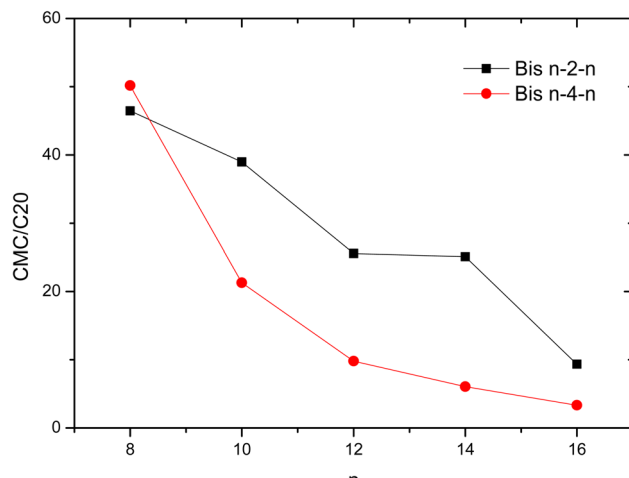
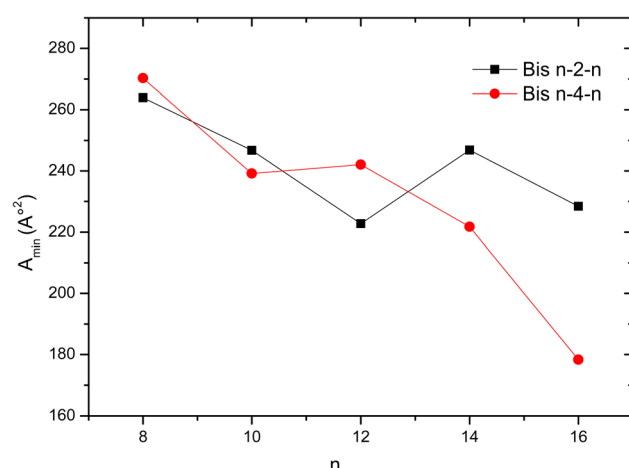


Fig. 3 Variation of surface tensions with the length of the alkyl chain.



Fig. 4 Variation of CMC/C₂₀ ratios with alkyl chain length.Fig. 5 Evolution of A_{\min} as a function of hydrophobic chain length.

carbon atoms, A_{\min} increases and even exceed that of gemini surfactants bearing a butylene spacer. This result can be explained by the arrangement of the spacer at the air–water interface.³⁷ Generally, a short spacer will adopt a fully extended conformation at the interface whereas a longer one will be more hydrophobic and flexible and tends to bend towards the air side of the interface to minimize the contact with water.⁴⁰ The latter conformation should result in a more compact organization where the head groups are closer to each other. This effect is more pronounced as the chain length increases, due to the increase in hydrophobic interactions between neighboring chains.

3.2.2. Conductivity. Conductivity measurements of surfactant solutions were also used to confirm the critical micellar concentrations and determine the ionization coefficients (α) and the standard free energies of micellization ΔG_{mic} (Table 1). A typical curve of the variation of the specific conductivity (K) as a function of the concentration of the compound **Bis 10–2–10** is shown as an example in Fig. S1.[†] The resulting CMC values are close to those measured by tensiometry and show a similar

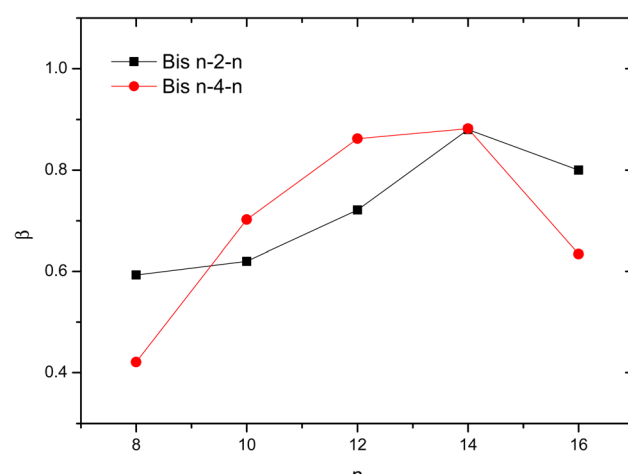
decreasing trend with the elongation of the hydrophobic chains (Fig. S2[†]).

The degrees of binding of counter ions to the micelles (β) were assessed using ionization coefficients (α), which were calculated from the ratio of slopes (dK/dC^{-1}) above and below the CMC. β was determined as $1 - \alpha$. The factor α measures the extent of dissociation of the counterions (Br^-) from the ammonium heads in the micelles while the parameter β is related to the counterions that are associated with the Stern layer to counteract the electrostatic repulsions between head-groups that prevent micelle formation. Below the CMC, the high concentration of free ions in solution leads to a rapid increase in the conductivity. As the micelles are formed, a slow increase in conductance is observed with the addition of surfactants due to the slow mobility of micelles and the reduction of the number of current carriers.⁴¹ A decrease in α (and therefore an increase in β) implies a neutralization of the charges on the micelle surface.

The variation of β values with the number of carbons in the hydrophobic chain is presented in Fig. 6. It was found that β increases with increasing hydrophobic chain length for $n = 8–14$ suggesting a decrease in micelle surface charge density. The counterion is tightly bound to the micellar aggregates, especially as the alkyl chain lengthens. A similar trend was obtained for conventional surfactant analogues.¹³ An increase in the number of micelles and/or the formation of a more compact micellar arrangement where the ammonium heads are strongly bound to counterions would be at the origin of this result.

An opposite behavior is obtained for longer hydrophobic chain $n = 16$. Similar result has already been reported in other works^{42–46} and was ascribed to the variation of the shape of formed micelles from ellipsoidal to spheroid.⁴⁶ Further Small Angle Neutron Diffraction (SANS) studies should be conducted to verify this hypothesis.

The dependence of β with spacer length is more complex. It was shown that the spacer's nature and length affect significantly the aggregation of gemini surfactants and the shape/size

Fig. 6 Variation of β values as a function of hydrophobic chain length n of gemini surfactants Bis n -s- n .

of the resulting aggregates.⁴⁷ Generally, the degree of binding of counter ions to micelles (β) tends to decrease with increasing spacer length.^{48,49} A short spacer induces strong electrostatic repulsions between head groups that are reduced by the condensation of larger amount of counterions at micelle surface resulting in increment in β .

This tendency seems to be verified only in the case of octyl and hexadecyl based surfactants (Fig. 6). Other factors as the hydrophobic interactions and the shape of the micelles should also modulate the extent of the association of the counter ions to the micelles.

The standard molar Gibbs energy of micellization ΔG_{mic} (kJ mol⁻¹) of the surfactants, which is the energy required to transfer one mole of surfactant from the water phase to the micellar pseudo-phase, was determined as follow:

$$\Delta G_{\text{mic}} = RT(0.5 + \beta)\ln X_{\text{CMC}}$$

Where X_{CMC} is the mole fraction of the CMC (mol L⁻¹): $X_{\text{CMC}} = \text{CMC}/55.4$ at 25 °C.

All surfactants showed a large negative ΔG_{mic} values indicating that the micellization is a thermodynamically favorable and spontaneous process. The energy of micellization decreases as the alkyl chain elongates until $n = 14$, suggesting that hydrophobic interactions govern the micellization process. ΔG_{mic} then slightly increases for the hexadecyl chain, likely due to steric hindrance caused by such a long chain (Fig. 7). For both series, the surfactants with tetradecyl chains (**Bis 14-n-14**) exhibit the lowest micellization energies and therefore have a great ability to form micelles in aqueous solution.

3.3. Antimicrobial activity

Gemini surfactants often exhibit a broad spectrum of biocidal activity. However, their antimicrobial mechanism is still not yet fully understood, probably due to the more complex molecular structures of this class of surfactants.⁵⁰ In addition to the classical mechanism of electrostatic/hydrophobic interactions of

cationic surfactants,¹³ other mechanisms based on the replacement of Mg²⁺ ions present in the pores of the *Escherichia coli* cell membrane by the ammonium heads of antimicrobial cationic gemini agents have also been reported. The larger size of the surfactant molecules as compared to Mg²⁺ ions causes swelling of the membrane. Following this step, respiratory enzymes are inhibited, and cell membrane components such as LPS and OmpE are released, leading to cell destruction.⁵¹ Similarly, it has been described that gemini bispyridinium salts tested on yeast *Saccharomyces cerevisiae* do not destroy the cell wall. Instead, they penetrate it and cause the internal organelle membranes to rupture.⁵²

The antimicrobial activity of gemini triazolic surfactants was assessed against two Gram-positive bacteria (*Staphylococcus Aureus* and *Bacillus subtilis*), two Gram-negative bacteria (*Escherichia coli* and *Pseudomonas aeruginosa*) and a fungus (*Aspergillus niger*). The tested concentrations ranged from 5–500 µg mL⁻¹. The obtained MIC and MBC values are collected in Table 2 and Fig. 8.

The results indicate that the triazolic surfactants are active against the investigated microorganism stains and exhibit mostly a bactericidal activity (BMC/MIC ≤ 4). The most active compound is **Bis 14-2-14** which enable the inhibition of bacteria and fungi growth at very low concentrations ranging from 7.03–28.12 µM and particularly against the biocide-resistant pathogenic *S. aureus* bacteria.

Overall, the investigated surfactants exhibit similar antimicrobial performance towards Gram-positive bacteria and fungi which often remains superior to that registered for Gram-negative bacteria. Similar behavior have been obtained for conventional triazolic ammonium surfactants and is ascribed to the inherent difference on cell composition of these microorganisms.¹³ In addition to peptidoglycan layers, common to both types of bacteria, that surround the cytoplasmic membrane, the Gram-negative bacteria, present an extra liposaccharides layer that hinders the penetration of hydrophobic molecules. Transport across this outer membrane is regulated as a function of surfactant's HLB.

The antimicrobial activity was closely tied to the length of the hydrophobic chain and spacer. Overall, tetradecyl and dodecyl chains promotes antimicrobial activity for **Bis n-2-n** and **Bis n-4-n** series, respectively. Short octyl chain seem also to be conducive for microorganism growth inhibition particularly for compound **Bis 8-4-8** which is active against *S. aureus* and *A. niger* with MIC values of 12.9 and 6.39 µM, respectively.

It is worth noting that the typical cut-off effect is not observed for the investigated gemini triazolic surfactants with a short spacer (Fig. 9). Instead, a substantial decrease in antimicrobial activity was observed for decyl and dodecyl chains. Usually, the MIC values of quaternary ammonium surfactants goes through a minimum for C₁₂–C₁₄ alkyl chain then increased gradually.⁵³ This trend is correlated to the increase of the hydrophobicity of surfactants, resulting in the enhancement of the hydrophobic interactions of their alkyl chains with the neighboring lipid chains of the bacterial membrane. The surfactant molecules will thus penetrate more readily into the membrane causing its destabilization and bacteria lysis.^{54–56}

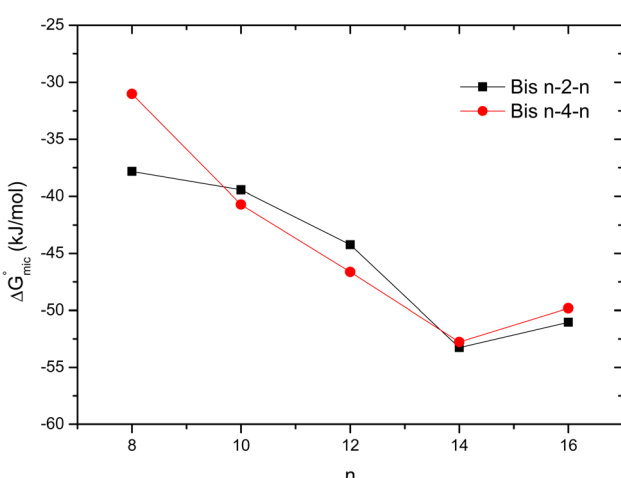


Fig. 7 Variation of Gibbs energy of micellization of gemini surfactants with the length of the hydrophobic chain.



Table 2 MIC values and MBC/MIC ratios measured for gemini surfactants

| Compounds | MIC ($\mu\text{mol L}^{-1}$) [MBC/MIC] | | | | |
|--------------------|--|--------------------------|-------------------------|-------------------------------|--------------------------|
| | <i>Staphylococcus aureus</i> | <i>Bacillus subtilis</i> | <i>Escherichia coli</i> | <i>Pseudomonas aeruginosa</i> | <i>Aspergillus niger</i> |
| Bis 8-2-8 | 20.31 [4] | 10.1 [4] | 81.25 [2] | 27.08 [4] | 20.31 [4] |
| Bis 10-2-10 | 149.84 [2] | 149.84 [2] | 149.84 [8] | 149.84 [4] | 75.00 [4] |
| Bis 12-2-12 | 139.03 [2] | 139.03 [4] | 139.03 [2] | 278.03 [4] | 139.03 [2] |
| Bis 14-2-14 | 7.03 [8] | 14.06 [2] | 14.06 [2] | 28.12 [8] | 14.06 [4] |
| Bis 16-2-16 | 108.05 [2] | 72.03 [4] | 144.07 [8] | 144.07 [16] | 72.03 [4] |
| Bis 8-4-8 | 12.90 [4] | 51.20 [2] | 51.20 [4] | 51.20 [4] | 6.39 [4] |
| Bis 10-4-10 | 56.90 [4] | 56.90 [4] | 56.90 [8] | 56.90 [4] | 56.90 [2] |
| Bis 12-4-12 | 62.12 [4] | 31.06 [4] | 31.06 [2] | 31.06 [8] | 31.06 [4] |
| Bis 14-4-14 | 116.14 [2] | 29.03 [2] | 116.14 [4] | 58.07 [4] | 58.07 [2] |
| Bis 16-4-16 | 141.75 [2] | 141.75 [8] | 425.25 [8] | 354.37 [16] | 141.75 [4] |

The hydrophilic/hydrophobic balance of **Bis n-2-n** compounds reported in this study bearing Intermediate-size chains ($n = 10-12$) seems to be not favorable to biocidal activity. The decrease in antibacterial activity of surfactants with a long alkyl chain ($>\text{C}_{14}$) is associated with their reduced solubility in water, which restricts their infiltration and transport across the cell membrane.

Regarding the effect of the spacer on the antimicrobial efficiency of the studied surfactants, two trends were obtained. For all microorganisms, **Bis n-4-n** showed lower MIC values than their **Bis n-2-n** counterparts for n ranging from 8 to 12 while an opposite behavior was noticed for $n = 14$ and 16. A peculiar result is obtained for compound **Bis 8-2-8** which exhibit a higher antibacterial activity as compared with **Bis 8-4-8** analogous towards *B. subtilis* and *P. aeruginosa* strains.

The MIC values of the triazolic geminis were compared to those reported in a previous study for single chain monomeric analogues CnTzTEA against *P. aeruginosa*, *B. subtilis*, and *A. niger* microorganisms. The results show that only **Bis 8-2-8**, **Bis 14-2-14**, and **Bis 8-4-8** exhibit similar or slightly better

antimicrobial activity.¹³ This finding is unexpected, since usually dimeric ammonium surfactants present enhanced biocidal activity due to two main factors: the presence of two positively charged ammonium heads that exacerbate the interaction with the negatively charged phospholipids outer membrane of bacteria and, the increased hydrophobic interactions of the two hydrophobic chains with the lipid bilayer membranes. Thus, the gemini surfactants often incorporate more readily in this membrane causing serious an irreversible damage to its integrity until the bacterial death.

Even if the lipid-surfactant interactions are mainly governed by the electrostatic forces, others works have shown that the number of ammonium heads is not the only determining factor in the bioactivity of gemini surfactants.⁵⁷ Other intrinsic structural factors of the surfactants are implied including the hydrophilic/lipophilic balance, the length of the hydrophobic alkyl chains and spacer, and the nature of the active groups present in the structure of the compounds.^{43,56}

It is worth mentioning that the investigated gemini surfactants are more effective against *P. aeruginosa* and *A. niger* than

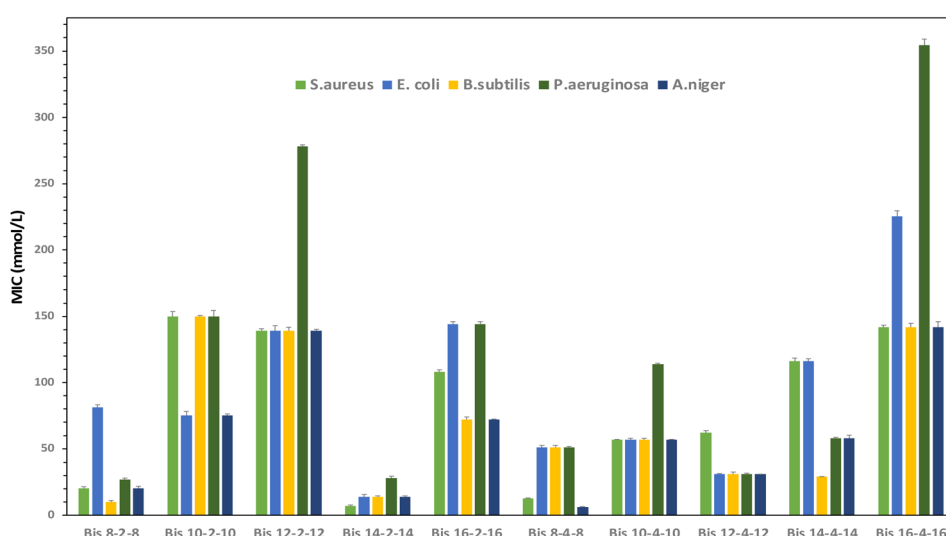


Fig. 8 MICs of gemini surfactants recorded against the microorganisms tested.



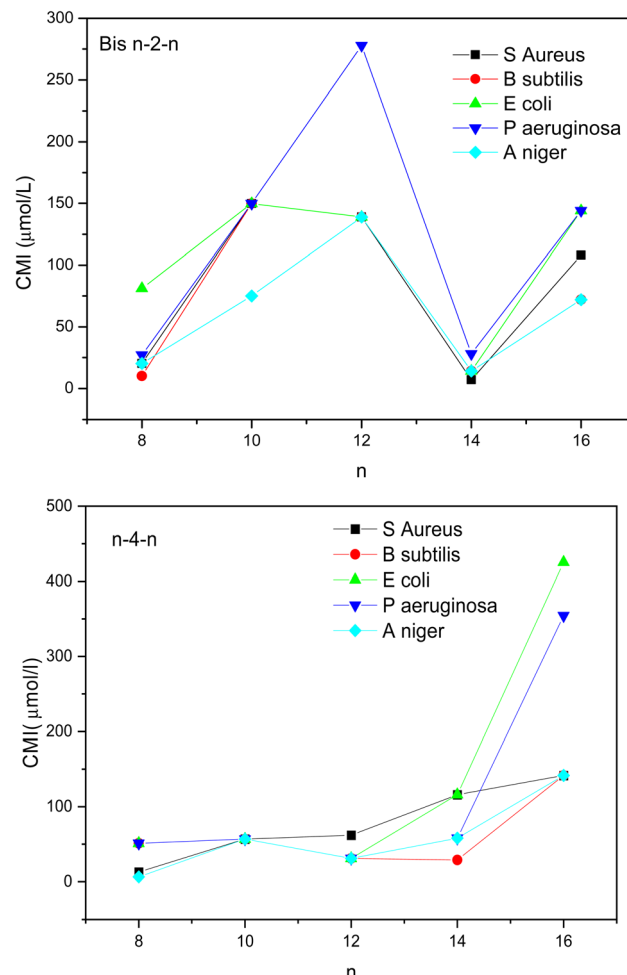


Fig. 9 Evolution of the MIC values of Bis n -s- n series according to the length of the alkyl chains.

benzalkonium chloride (BAC), which is currently used for hospital disinfection ($\text{MIC}(\text{BAC}) = 175.0 \mu\text{M}$,⁵⁸ $78.1 \mu\text{M}$,⁵⁹ for *P. aeruginosa*, and *A. niger*, respectively). Compound **Bis 14-2-14** demonstrated additional antimicrobial activity against *E. coli* with a MIC of $14.06 \mu\text{M}$, lower than that reported for BAC ($19.5 \mu\text{M}$).⁶⁰

Bis n -s- n compounds exhibited also antimicrobial performance comparable to or higher than that of previously reported Gemini bisQuat type surfactants with aliphatic or aromatic spacers.⁶¹ **Bis 14-2-14**, in particular, showed stronger activity against *E. coli* with a MIC of $14.06 \mu\text{M}$ ($11.71 \mu\text{g mL}^{-1}$) compared to the hydrocarbon analog gemini 14-2-14 (MIC = $500 \mu\text{g mL}^{-1}$).⁵⁶

4 Conclusion

A new series of Gemini quaternary ammonium surfactants bearing alkyl chains and a spacer arm of varying lengths has been reported in the present work. A systematic study of the surface properties of these compounds in aqueous solution was carried out by tensiometry and conductometry. We have shown that all gemini surfactants form aggregates at lower

concentrations than conventional surfactants for the same alkyl chain length. The lengthening of the hydrophobic alkyl chain from 8 to 16 carbons and the use of short spacer causes a decrease in the critical micellar concentration value of gemini surfactants. The triazole ring is also an important structural parameter in aggregation phenomena and contributes positively to the micellization process.

Antimicrobial examination of both sets of geminis revealed strong antimicrobial activity for many compounds, with MIC levels ranging from 6.39 to $81 \mu\text{M}$, particularly for compounds with octyl or tetradecyl side-chains. The remaining compounds showed moderate activity, with MIC values of 150 – $354 \mu\text{M}$.

It is noteworthy that the compound **Bis 14-2-14** demonstrated simultaneous efficacy against microscopic fungi, Gram-positive bacteria *B. subtilis* and *S. aureus*, as well as Gram-negative bacteria, *E. coli* and *P. aeruginosa*. The latter microorganism is often resistant to many antimicrobial agents and frequently forms biofilms on various surfaces in the cosmetic, food, and medical sectors. This antimicrobial multi-activity is encouraging for the development of future series of functional surfactants.

Author contributions

Mechken Karima Amel: investigation, visualization, methodology, writing – original draft. Mohammed Menouar: investigation, Zahera Talbi: investigation. Salima Saidi-Besbes: conceptualization, supervision, resources, funding acquisition, writing – review & editing. Moulay Belkhodja: resources.

Conflicts of interest

The author(s) confirm that this article content has no conflicts of interest.

Acknowledgements

This work was supported by the General Directorate for Scientific Research and Technological Development (DGRSDT) and the Ministry of Higher Education and Scientific Research of Algeria.

References

- 1 F. M. Menger and J. S. Keiper, Gemini surfactants, *Angew. Chem., Int. Ed.*, 2000, **39**, 1906–1920.
- 2 S. He, X. Liu, P. Yan, A. Wang, J. Su and X. Su, Preparation of gemini surfactant/graphene oxide composites and their superior performance for Congo red adsorption, *RSC Adv.*, 2019, **9**, 4908–4916.
- 3 W. Zhang, G. Huang, J. Wei, H. Li, R. Zheng and Y. Zhou, Removal of phenol from synthetic waste water using Gemini micellar-enhanced ultrafiltration (GMEUF), *J. Hazard. Mater.*, 2012, **235**, 128–137.
- 4 T. Mao, H. Huang, D. Liu, X. Shang, W. Wang and L. Wang, Novel cationic Gemini ester surfactant as an efficient and





eco-friendly corrosion inhibitor for carbon steel in HCl solution, *J. Mol. Liq.*, 2021, **339**, 117174.

5 Y. Wang, J. Yan, Z. Li, X. Liu, X. Zhang, L. Wei and S. Ye, Construction of Gemini composite based on TiO₂ pillared montmorillonite for efficient oil–water separation, *Appl. Surf. Sci.*, 2023, **612**, 155977.

6 J. Xiao, L. Wang, H. Z. N. Ma, M. Tao and W. Zhang, Immobilization of Pd(0) nanoparticles on gemini quaternary ammonium functionalized polyacrylonitrile fibers as highly active catalysts for heck reactions and 4-nitrophenol reduction, *Chem. Eng. Sci.*, 2022, **247**, 117053.

7 E. A. Badr, S. H. Shafeek, H. H. H. Hefni, A. M. Elsharif, A. A. Alanezi, S. M. Shaban and D.-H. Kim, Synthesis of Schiff base-based cationic Gemini surfactants and evaluation of their effect on *in situ* AgNPs preparation: Structure, catalytic, and biological activity study, *J. Mol. Liq.*, 2021, **326**, 115342.

8 D. Liu, X. Weng, Y. Jin, R. M. Kasomo, S. Ao and H. Li, Removal of feldspar from phosphate ore using Gemini quaternary ammonium salt as a novel collector, *Colloids Surf., A*, 2022, **644**, 128821.

9 D. R. Karsa, *Surfactants in Polymers, Coatings, Inks, and Adhesives*, CRC Press, 2020.

10 Z. Yaseen, V. K. Aswal and A. A. Dar, Rheological response and small-angle neutron-scattering study of diester-bonded cationic biodegradable gemini surfactants in presence of different additives, *Colloid Polym. Sci.*, 2014, **292**, 3113–3125.

11 B. E. Brycki, I. H. Kowalczyk, A. Szulc, O. Kaczerewska and M. Pakiet, Multifunctional gemini surfactants: structure, synthesis, properties and applications, *Appl. Charact. Surfactants*, 2017, 97–155.

12 M. Zhou, J. Huang, Y. Zhao, X. Deng, R. Ni, Y. Zhao and Y. He, Synthesis and Physicochemical Properties of CO₂-switchable Gemini Surfactants, *J. Mol. Liq.*, 2022, **352**, 118642.

13 K. A. Mechken, M. Menouar, M. Belkhodja and S. Saidi-Besbes, Synthesis, Surface Properties and Bioactivity of Novel 4-Substituted 1, 2, 3-Triazole Quaternary Ammonium Surfactants, *J. Mol. Liq.*, 2021, **338**, 116775.

14 G. Wang, L. Liu, D. He, R. Lu, Y. Xie and L. Lai, Cationic-anionic surfactant mixtures based on gemini surfactant as a candidate for enhanced oil recovery, *Colloids Surf., A*, 2023, **677**, 132297.

15 M. E. Ahmed, A. S. Sultan, M. S. Kamal, T. Saikia, M. Mahmoud, S. Patil and M. Kanj, Relationship between Dynamic Interfacial Tension and Ultimate Recovery in Gemini Surfactant Flooding: An Exploration through Fractured Micromodels, *Energy Fuels*, 2023, **37**, 11787–11796.

16 S. M. Shaban, J. Kang and D.-H. Kim, Surfactants: Recent advances and their applications, *Compos. Commun.*, 2020, **22**, 100537.

17 R. Aggrawal, S. Halder, S. Dyagala and S. K. Saha, Refolding of denatured gold nanoparticlesconjugated bovine serum albumin through formation of catanions between gemini surfactant and sodium dodecyl sulphate, *RSC Adv.*, 2022, **12**, 16014–16028.

18 H. Lal and M. Akram, Physico-chemical characterization of bovine serum albumin-cationic gemini surfactant interaction, *J. Mol. Liq.*, 2022, **361**, 119626.

19 J. A. S. Almeida, E. F. Marques, A. S. Jurado and A. A. C. C. Pais, The effect of cationic gemini surfactants upon lipidmembranes. An experimental and molecular dynamics simulation study, *Phys. Chem. Chem. Phys.*, 2010, **12**, 14462–14476.

20 A. Shaheen and R. Arif, Synthesis, micellization behaviour and cytotoxic properties of imidazolium-based gemini surfactants, *Colloid Interface Sci. Commun.*, 2020, **36**, 100257.

21 J. Aslam, I. H. Lone, F. Ansari, A. Aslam, R. Aslam and M. Akram, Molecular binding interaction of pyridinium based gemini surfactants with bovine serum albumin: Insights from physicochemical, multispectroscopic, and computational analysis, *Spectrochim. Acta, Part A*, 2021, **250**, 119350.

22 B. Cai, X. Li, Y. Yang and J. Dong, Surface properties of Gemini surfactants with pyrrolidinium head groups, *J. Colloid Interface Sci.*, 2012, **370**, 111–116.

23 L. Pérez, A. Pinazo, R. Pons and M. Infante, Gemini surfactants from natural amino acids, *Adv. Colloid Interface Sci.*, 2014, **205**, 134–155.

24 M. Zhou, Y. Chen, J. Zou and J. Bu, Recent advances in the synthesis of sulfonate gemini surfactants, *J. Surfactants Deterg.*, 2018, **21**, 443–453.

25 S. Datta, J. Biswas and S. Bhattacharya, How does spacer length of imidazolium gemini surfactants control the fabrication of 2D-Langmuir films of silver-nanoparticles at the air–water interface?, *J. Colloid Interface Sci.*, 2014, **430**, 85–92.

26 T. Lu, Y. Lan, C. Liu, J. Huang and Y. Wang, Surface properties, aggregation behavior and micellization thermodynamics of a class of gemini surfactants with ethyl ammonium headgroups, *J. Colloid Interface Sci.*, 2012, **377**, 222–230.

27 L. Wang, Y. Zhang, L. Ding, J. Liu, B. Zhao, Q. Deng and T. Yan, Synthesis and physicochemical properties of novel gemini surfactants with phenyl-1,4-bis(carbamoylmethyl) spacer, *RSC Adv.*, 2015, **5**, 74764–74773.

28 S. M. S. Hussain, M. S. Kamal, T. Solling, M. Murtaza and L. T. Fogang, Surface and thermal properties of synthesized cationic poly(ethylene oxide) gemini surfactants: the role of the spacer, *RSC Adv.*, 2019, **9**, 30154–30163.

29 F. E.-T. Heakal and A. E. Elkholly, Gemini surfactants as corrosion inhibitors for carbon steel, *J. Mol. Liq.*, 2017, **230**, 395–407.

30 D.-Y. Zhu, F. Cheng, Y. Chen and S.-C. Jiang, Preparation, characterization and properties of anionic gemini surfactants with long rigid or semi-rigid spacers, *Colloids Surf., A*, 2012, **397**, 1–7.

31 D. R. Mundhada and A. V Chandewar, An Overview on Cationic Surfactant, *Res. J. Pharm. Dos. Technol.*, 2015, **7**, 294.

32 Y. Xie and X. He, Asymmetric Gemini surfactants as corrosion inhibitors for carbon steel in acidic medium:

Experimental and theoretical studies, *Colloids Surf., A*, 2023, **660**, 130850.

33 C. Menendez, A. Chollet, F. Rodriguez, A. Inard, M. R. Pasca, C. Lherbet and M. Baltas, Chemical synthesis and biological evaluation of triazole derivatives as inhibitors of InhA and antituberculosis agents, *Eur. J. Med. Chem.*, 2012, **52**, 275–283.

34 M. Balouiri, M. Sadiki and S. K. Ibnsouda, Methods for *in vitro* evaluating antimicrobial activity: A review, *J. Pharm. Anal.*, 2016, **6**, 71–79.

35 K. Taleb, M. Mohamed-Benkada, N. Benhamed, S. Saidi-Besbes, Y. Grohens and A. Derdour, Benzene ring containing cationic gemini surfactants: Synthesis, surface properties and antibacterial activity, *J. Mol. Liq.*, 2017, **241**, 81–90.

36 C. Benbayer, S. Saidi-Besbes, E. T. de Givenchy, S. Amigoni, F. Guittard and A. Derdour, Investigation of structure–surface properties relationship of semi-fluorinated polymerizable cationic surfactants, *J. Colloid Interface Sci.*, 2013, **408**, 125–131.

37 K. Taleb, I. Pillin, Y. Grohens and S. Saidi-Besbes, Gemini surfactant modified clays: Effect of surfactant loading and spacer length, *Appl. Clay Sci.*, 2018, **161**, 48–56.

38 A. Laatiris, M. El Achouri, M. R. Infante and Y. Bensouda, Antibacterial activity, structure and CMC relationships of alkanediyl α , ω -bis (dimethylammonium bromide) surfactants, *Microbiol. Res.*, 2008, **163**, 645–650.

39 M. J. Rosen, L. Fei, Y. Zhu and S. W. Morrall, The Relationship of the Environmental Effect of Surfactants to Their Interfacial Properties, *J. Surfactants Deterg.*, 1999, **2**, 343–347.

40 X. Zhong, J. Guo, L. Feng, X. Xu and D. Zhu, Cationic Gemini surfactants based on adamantane: synthesis, surface activity and aggregation properties, *Colloids Surf., A*, 2014, **441**, 572–580.

41 S. Afzal, M. S. Lone, N. Nazir and A. A. Dar, pH Changes in the Micelle–Water Interface of Surface-Active Ionic Liquids Dictate the Stability of Encapsulated Curcumin: An Insight Through a Unique Interfacial Reaction between Arenediazonium Ions and *t*-Butyl Hydroquinone, *ACS Omega*, 2021, **6**, 14985–15000.

42 A. Bhadani and S. Singh, Synthesis and properties of thioether spacer containing gemini imidazolium surfactants, *Langmuir*, 2011, **27**, 14033–14044.

43 I. Kowalczyk, M. Pakiet, A. Szulc and A. Koziróg, Antimicrobial Activity of Gemini Surfactants with Azapolymethylene Spacer, *Molecules*, 2020, **25**, 4054.

44 A. Pinazo, R. Pons, M. Bustelo, M. A. Manresa, C. Moran, M. Raluy and L. Perez, Gemini histidine based surfactants: Characterization; surface properties and biological activity, *J. Mol. Liq.*, 2019, **289**, 111156.

45 L. D. Song and M. J. Rosen, Surface properties, micellization, and premicellar aggregation of gemini surfactants with rigid and flexible spacers, *Langmuir*, 1996, **12**, 149–1153.

46 J. Hoque, S. Gonuguntla, V. Yarlagadda, V. K. Aswal and J. Haldar, Effect of amide bonds on the self-assembly of gemini surfactants, *Phys. Chem. Chem. Phys.*, 2014, **16**, 11279–11288.

47 Y. Han and Y. Wang, Aggregation behavior of gemini surfactants and their interaction with macromolecules in aqueous solution, *Phys. Chem. Chem. Phys.*, 2011, **13**, 1939–1956.

48 M. Frindi, B. Michels, H. Levy and R. Zana, Alkanediyl-alpha, omega -bis (dimethylalkylammonium bromide) Surfactants. 4. Ultrasonic absorption studies of amphiphile exchange between micelles and bulk phase in aqueous micellar solution, *Langmuir*, 1994, **10**, 1140–1145.

49 V. I. Martín, A. Rodríguez, M. del M. Graciani, I. Robina and M. L. Moyá, Study of the micellization and micellar growth in pure alkanediyl- α - ω -bis (dodecyldimethylammonium) bromide and MEGA10 surfactant solutions and their mixtures. Influence of the spacer on the enthalpy change accompanying sphere-to-rod transitions, *J. Phys. Chem. B*, 2010, **114**, 7817–7829.

50 D. Kwaśniewska, Y.-L. Chen and D. Wieczorek, Biological activity of quaternary ammonium salts and their derivatives, *Pathogens*, 2020, **9**, 459.

51 T. Sumitomo, T. Maeda, H. Nagamune and H. Kourai, Bacterioclastic action of a bis-quaternary ammonium compound against *Escherichia coli*, *Biocontrol Sci.*, 2004, **9**, 1–9.

52 A. Shirai, T. Sumitomo, M. Kurimoto, H. Maseda and H. Kourai, The mode of the antifungal activity of gemini-pyridinium salt against yeast, *Biocontrol Sci.*, 2009, **14**, 13–20.

53 P. Gilbert and L. E. Moore, Cationic antiseptics: diversity of action under a common epithet, *J. Appl. Microbiol.*, 2005, **99**, 703–715.

54 K. Kuperkar, J. Modi and K. Patel, Surface-active properties and antimicrobial study of conventional cationic and synthesized symmetrical gemini surfactants, *J. Surfactants Deterg.*, 2012, **15**, 107–115.

55 K. Cook, K. Tarnawsky, A. J. Swinton, D. D. Yang, A. S. Senetra, G. A. Caputo, B. R. Carone and T. D. Vaden, Correlating lipid membrane permeabilities of imidazolium ionic liquids with their cytotoxicities on yeast, bacterial, and mammalian cells, *Biomolecules*, 2019, **9**, 251.

56 S. Zhang, S. Ding, J. Yu, X. Chen, Q. Lei and W. Fang, Antibacterial activity, *in vitro* cytotoxicity, and cell cycle arrest of gemini quaternary ammonium surfactants, *Langmuir*, 2015, **31**, 12161–12169.

57 T. J. Paniak, M. C. Jennings, P. C. Shanahan, M. D. Joyce, C. N. Santiago, W. M. Wuest and K. P. C. Minbile, The antimicrobial activity of mono-, bis-, tris-, and tetracationic amphiphiles derived from simple polyamine platforms, *Bioorg. Med. Chem. Lett.*, 2014, **24**, 5824–5828.

58 S. Q. Fu, J. W. Guo, X. Zhong, Z. Yang and X. F. Lai, Synthesis, physicochemical property and antibacterial activity of gemini quaternary ammonium salts with a rigid spacer, *RSC Adv.*, 2016, **6**, 16507–16515.

59 S. El Hage, B. Lajoie, J. L. Stigliani, A. Furiga-Chusseau, C. Roques and G. Baziard, Synthesis, Antimicrobial activity and physico-chemical properties of some *n*-



alkyldimethylbenzylammonium halides, *J. Appl. Biomed.*, 2014, **12**, 245–253.

60 S. El Hage, B. Lajoie, J.-L. Stigliani, A. Furiga-Chusseau, C. Roques and G. Baziard, Synthesis, antimicrobial activity and physico-chemical properties of some *n*-alkyldimethylbenzylammonium halides, *J. Appl. Biomed.*, 2014, **12**, 245–253.

61 B. Brycki, A. Koziróg, I. Kowalczyk, T. Pospieszny, P. Materna and J. Marciniak, Synthesis, structure, surface and antimicrobial properties of new oligomeric quaternary ammonium salts with aromatic spacers, *Molecules*, 2017, **22**, 1810.

